

# Resonance Scattering in Optical Lattices and Molecules: Interband versus Intraband Effects

Xiaoling Cui<sup>1</sup>, Yupeng Wang<sup>1</sup> and Fei Zhou<sup>2</sup>

<sup>1</sup>*Beijing National Laboratory for Condensed Matter Physics and Institute of Physics,  
Chinese Academy of Sciences, Beijing 100190, China*

<sup>2</sup>*Department of Physics and Astronomy, The University of British Columbia, Vancouver, B. C., Canada V6T1Z1*  
(Dated: May 30, 2019)

We study the low-energy two-body scattering in optical lattices with all higher-band effects included in an effective potential, using a renormalization group approach. As the potential depth reaches a certain value, a resonance of low energy scattering occurs even when the negative s-wave scattering length ( $a_s$ ) is much shorter than the lattice constant. These resonances can be mainly driven either by interband or intraband effects or by both, depending on the magnitude of  $a_s$ . Furthermore the low-energy scattering matrix in optical lattices has a much stronger energy-dependence than that in free space. We also investigate the momentum distribution for molecules when released from optical lattices.

For a dilute ultracold atomic gas, the two-body s-wave scattering length  $a_s$  is known to be conveniently tunable via magnetic-field-induced Feshbach resonances[1, 2]. Experimentally in the presence of external trapping confinements, however, binary atomic collision properties can be dramatically modified as revealed both theoretically and experimentally in three-dimensional (3D) harmonic traps[3, 4, 5], and in 1D waveguides[6, 7]. More remarkably, the waveguides confinement can further result in very peculiar effective potentials as pointed out in a few early papers[6, 8]. Especially, Olshanii et al. systematically studied scattering between atoms in a 1D waveguide and pointed out that the effective potential for atoms in the lowest transverse mode can reach the hardcore limit; in fact, this occurs when  $a_s$  is positive and comparable to  $a_{\perp}$ , the confinement length along the transverse direction.

Interacting atoms in optical lattices are another subject that has attracted enormous interests for the past few years[9, 10, 11]. However, till now what happens to binary collisions in an optical lattice and scattering between two Bloch states on the other hand have not been thoroughly studied and the subject of molecules of Bloch waves is not well understood. Given the growing number of experiments on interacting atoms in optical lattices, it is becoming essential to understand the fundamentals of two-body scattering and other few-body physics of Bloch states. These systematic analyses should form corner stones of many-body theories on scattering atoms and set potential benchmarks for future quantitative calculations of interaction parameters appearing in many-body Hamiltonians, especially when multiple band physics is relevant. These studies can further cast light on dynamics of colliding atoms or condensates in optical lattices and motivate more experiments on this subject. Our calculations also suggest an alternative way of creating cold molecules with robust structures that only depend on lowest band physics in optical lattices (see below). Finally, these results will provide guidelines for quantum

information processors that involve manipulation or precise control of scattering atoms in optical lattices[12].

Scattering near the bottom of the lowest band in an optical lattice was also previously studied and resonance scattering was pointed out for attractive interactions[13]. However, studies there were carried out in a single-band approximation that is only justifiable for deep lattices; effects of higher bands were not included. In this work we are going to develop an approach which is generally valid for all potential depths or free space scattering lengths and which allows us to quantify full effects of the lowest band and higher bands. Our main proposal is to evaluate the effective potential for atoms in the lowest band that takes into account multiple virtual scattering processes involving *higher bands*. We then apply this renormalized potential to calculate  $T$ -matrix of low-energy scattering. In optical lattices, full solutions to scattering waves in the real space representation are technically more difficult to obtain than those in waveguides studied previously. A related issue is the complexity of interaction matrix elements, which make multiple scattering processes quite challenging to track. These obstacles can be effectively overcome by employing a numerical momentum shell renormalization that has been carried out to obtain effective potentials. To our knowledge, this is the first systematic theoretical attempt to reveal how Bloch waves are scattered in optical lattices at arbitrary laser intensities.

We have examined the low-energy effective scattering between Bloch waves. When free space scattering lengths  $a_s (< 0)$  are comparable to or larger than the lattice constant  $a_L (\sim 400nm)$ , switching on optical lattices can quickly drive the system to a resonance. For most alkali atoms practically this type of resonance scattering can only occur when pre-tuned to close to Feshbach resonances; and interband scattering to higher bands contributes substantially to the lowest-band effective potential. In addition, another class of resonances can occur uniquely in optical lattices when magnitudes of scattering

lengths  $a_s (< 0)$  are arbitrarily small. In this case, scattering at the bottom of the lowest band is predominately driven by *intra*band multiple scattering to the mid of the band. The effective two-body potential is barely affected by higher bands and resonances are mainly attributed to the enhanced effective masses of atoms in optical lattices. This feature of resonances is also distinctly different from that in waveguides, where higher energy channels are necessarily involved but the effective mass is the same as the bare one. If we view the large effective mass of atoms in optical lattices as a consequence of dressing bare atoms with laser photons, these resonances actually occur between strongly dressed atoms and corresponding bound states are molecules of dressed atoms.

To facilitate the discussion on the low-energy scattering atoms, we start with a two-body Hamiltonian

$$H = \sum_{\alpha} \epsilon_{\alpha} |\alpha\rangle \langle \alpha| + \sum_{\alpha\beta} U_{\alpha\beta} |\alpha\rangle \langle \beta|, \quad (1)$$

with  $|\alpha(\beta)\rangle$  being arbitrary two-body scattering states. For scattering in free space with a short range potential approximated as  $U(\mathbf{r}) = U_0 \delta^3(\mathbf{r})$ ,  $|\alpha\rangle, |\beta\rangle = |\mathbf{k}, -\mathbf{k}\rangle$  and  $U_{\alpha\beta} = \frac{U_0}{\Omega}$  with  $\Omega$  the volume; to obtain an effective low-energy Hamiltonian, we employ the momentum-shell renormalization group(RG) equation approach[14]. The key idea here is at an arbitrary cut-off momentum  $\Lambda$ , we can further divide the  $\mathbf{k}$ -space into two regions, i.e., a core region defined by  $|\mathbf{k}| < \Lambda - \delta\Lambda$  and a shell  $\Lambda - \delta\Lambda < |\mathbf{k}| < \Lambda$ . Correspondingly, we split the Hamiltonian at a given cutoff  $\Lambda$  into three pieces  $H(\Lambda) = H^< + H^> + H^{><}$  which respectively describe interacting atoms within the core, within the shell and the scattering in between. For atoms with  $|\mathbf{k}| \ll \Lambda$ , the second-order virtual scattering into high energy states within the shell caused by  $H^{><}$  modifies the low-energy scattering amplitudes and results in a correction ( $\delta U$ ) in  $H^<$ . One can then obtain a differential RG equation for  $U$  in terms of the cut-off momentum  $\Lambda$ ,

$$\frac{1}{U^2} \frac{\delta U}{\delta \Lambda} = \frac{1}{\Omega} \frac{\delta}{\delta \Lambda} \left( \sum_{|\mathbf{k}| < \Lambda} \frac{1}{2\epsilon_{\mathbf{k}}} \right). \quad (2)$$

So the effective potential  $U$  for scattering atoms at momenta smaller than  $\Lambda$  is renormalized due to the coupling to virtual states at larger momenta and is given as

$$\frac{1}{U(\Lambda)} = \frac{1}{U(\Lambda^*)} + \frac{1}{\Omega} \sum_{\Lambda < |\mathbf{k}| < \Lambda^*} \frac{1}{2\epsilon_{\mathbf{k}}}. \quad (3)$$

Boundary conditions  $U(\Lambda^*) = U_0$  and  $U(0) = T_0$  relate  $U_0$  to the low-energy scattering length  $a_s (= \frac{mT_0}{4\pi})$  via  $\frac{m}{4\pi a_s} = \frac{1}{U_0} + \frac{1}{\Omega} \sum_{|\mathbf{k}| < \Lambda^*} \frac{1}{2\epsilon_{\mathbf{k}}}$ . ( $\Lambda^*$  is an ultraviolet momentum cut-off that is set by the range of interactions.)

One can apply a similar idea to optical lattices. For a cubic optical lattice with potential  $V(\mathbf{r}) = V_0 \sum_i \sin^2(2\pi x_i/\lambda)$  and spacing  $a_L = \lambda/2$ , Bloch states

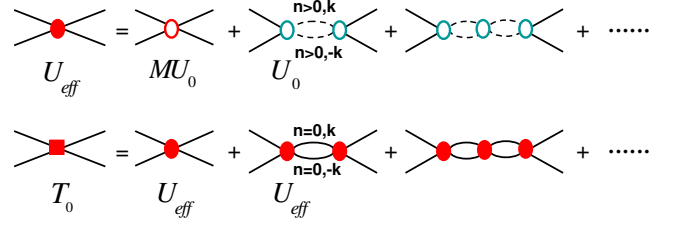


FIG. 1: (color online). A RG approach to scattering in optical lattices. Various two-particle vertex functions are indicated below the corresponding diagrams. Dashed (solid) lines between two vertices represent states in the lowest  $n = 0$  band (higher  $n > 0$  bands).

$\phi_{n\mathbf{k}}(\mathbf{r}) = \frac{1}{\sqrt{\Omega}} \sum_{\mathbf{G}} w_n(\mathbf{k} + \mathbf{G}) e^{i(\mathbf{k} + \mathbf{G}) \cdot \mathbf{r}}$  and energies  $\epsilon_{n\mathbf{k}}$  can be numerically obtained; here  $n$  are band indices;  $\mathbf{k} \in BZ$  (Brillouin zone) and  $\mathbf{G}$  is the reciprocal lattice vector; eigenvector element  $w_n(\mathbf{q})$  is related to the Wannier wavefunction in momentum space. It is also convenient to specify potential depth  $V_0$  in units of the recoil energy  $E_R = \frac{\pi^2 \hbar^2}{2ma_L^2}$  via a dimensionless quantity  $v = \frac{V_0}{E_R}$ .

First we calculate the interaction matrix element between Bloch states  $|\alpha\rangle = |\{n_1, \mathbf{k}\}, \{n_2, -\mathbf{k}\}\rangle$  and  $|\beta\rangle = |\{n'_1, \mathbf{k}'\}, \{n'_2, -\mathbf{k}'\}\rangle$ ,

$$U_{\alpha\beta} \equiv \langle \alpha | U | \beta \rangle = \frac{U_0}{\Omega} \sum_{\mathbf{Q}} M_{\alpha}^{\mathbf{Q}} * M_{\beta}^{\mathbf{Q}}, \quad (4)$$

here  $M_{\alpha}^{\mathbf{Q}} = \sum_{\mathbf{G}} w_{n_1}(\mathbf{k} + \mathbf{G}) w_{n_2}(\mathbf{Q} - \mathbf{k} - \mathbf{G})$ . Calculations of  $U_{\alpha\beta}$  indicate that: a) interactions involving incident and scattered particles both in the lowest band, given as  $MU_0$ [15], dominate all matrix elements; b) the next dominating contributions that are approximately equal to  $U_0$  as in the free space, include two kinds of processes, i.e., two particles in the lowest band scattered to a single higher band or two in the same higher band scattered to the original or another higher band; c) interactions involving two incident or scattered particles in two different bands contribute the least and therefore are neglected in this work.

In view of these features of  $U_{\alpha\beta}$  and following the idea outlined before Eq.(3), we obtain the effective potential  $U_{eff}$  for the lowest band and further calculate the scattering potential  $T_0$  for states near  $\epsilon_{n\mathbf{k}} = 0$ , as diagrammatically shown in Fig.1, to be

$$\begin{aligned} \frac{1}{U_{eff}} &= \frac{m\eta}{4\pi a_L M} \left( \frac{a_L}{a_s} - C_1 \right), \\ \frac{1}{T_0} &= \frac{m\eta}{4\pi a_L M} \left( \frac{a_L}{a_s} - C_1 + C_2 \right), \end{aligned} \quad (5)$$

with

$$\begin{aligned} C_1 &= \frac{4\pi a_L}{m\Omega} \left( \sum_{\mathbf{k}} \frac{1}{2\epsilon_{\mathbf{k}}} - \sum_{n>0, \mathbf{k}} \frac{1}{2\epsilon_{n\mathbf{k}}} \right), \\ C_2 &= \frac{4\pi a_L}{m\Omega} \sum_{n=0, \mathbf{k}} \frac{M}{\eta} \frac{1}{2\epsilon_{n\mathbf{k}}}, \end{aligned} \quad (6)$$

here  $\eta = (1 + (1 - \frac{1}{M})\frac{U_0}{\Omega} \sum_{n>0, \mathbf{k}} \frac{1}{2\epsilon_{n\mathbf{k}}})^{-1}$  is close to unity in the regions that interest us[16]; evidently  $C_1$  and  $C_2$  are respectively ascribed to interband and intraband scattering effects.

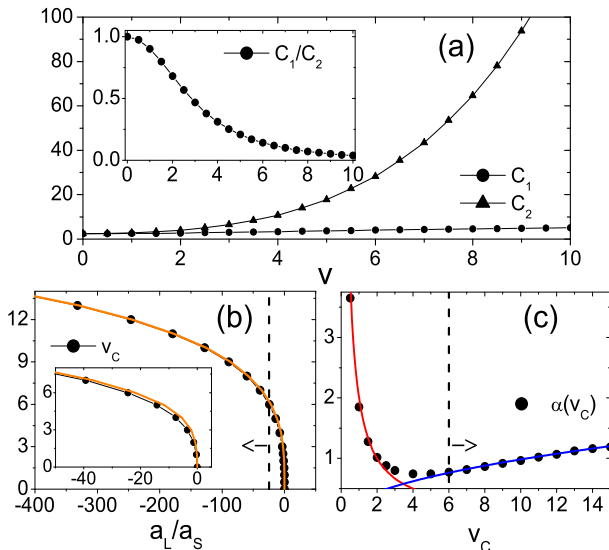


FIG. 2: (color online). (a) Interband ( $C_1$ ) and intraband ( $C_2$ ) effects vs lattice potentials  $v$ . Inset shows the ratio. (b) Resonance lattice potentials  $v_c$  vs  $a_L/a_s$ . The orange line shows results without  $\eta = 1$  approximation. Inset is the magnified plot where deviations are relatively visible. (c)  $\alpha(v_c)$  near resonance. Red and blue lines are fit to  $\frac{2}{v_c}$  and  $\frac{2}{\pi\lambda}\sqrt{v_c}$  respectively. Dashed line and arrow in both (b) and (c) locate the region,  $a_L/a_s < -24.5$  and  $v_c > 6$ , where intraband scattering processes dominate over interband ones.

Our main results are shown in Fig.2. At  $v = 0$  and  $M = 1$  we reproduce the free space result  $T_0 = 4\pi a_s/m$ . With increasing  $v$ , the intraband scattering gradually takes a dominating role over other ones, reflected by a much more rapid increase of  $C_2$  than  $C_1$ . For instance at  $v = 5$ ,  $C_1/C_2 = 0.21$ . In the large  $v$  limit, with the lowest band spectrum  $\epsilon_{\mathbf{k}} = t \sum_i (1 - \cos k_i a_L)$ ,  $t$  being the hopping amplitude, we find that

$$C_1 = \sqrt{8}v^{\frac{1}{4}}, \quad C_2 = \frac{\pi\gamma}{32\sqrt{2}}e^{2\sqrt{v}} \quad (\gamma \approx 4). \quad (7)$$

To obtain Bloch wave scattering length  $a_{\text{bloch}}$  we first introduce an effective (band) mass  $m_{\text{eff}} = 1/\frac{\partial^2 \epsilon_{n\mathbf{k}}}{\partial k^2}|_G$  and relate it to the scattering potential  $T_0 = 4\pi a_{\text{bloch}}/m_{\text{eff}}$ . For a negative  $a_s$ , the resonance ( $a_{\text{bloch}} \rightarrow \infty$ ) occurs at lattice potential  $v_c$  when  $\frac{a_L}{a_s} = -(C_2 - C_1)$ . Across resonance,  $a_{\text{bloch}}$  obeys an asymptotic equation

$$\frac{a_{\text{bloch}}}{a_L} = \frac{\alpha(v_c)}{v - v_c}. \quad (8)$$

In the limit of  $|a_s| \ll a_L$ ,  $v_c$  and  $\alpha$  can be estimated using Eq.(7); in the opposite limit, they can be obtained using

the perturbation theory with respect to  $v$ ,

$$|a_s| \ll a_L : \quad v_c = \frac{1}{4} \ln^2 \left( \frac{32\sqrt{2}}{\pi\gamma} \frac{a_L}{|a_s|} \right), \quad \alpha = \frac{2}{\pi\gamma} \sqrt{v_c};$$

$$|a_s| \gg a_L : \quad v_c = 2\sqrt{\frac{a_L}{|a_s|}}, \quad \alpha = \frac{2}{v_c}.$$

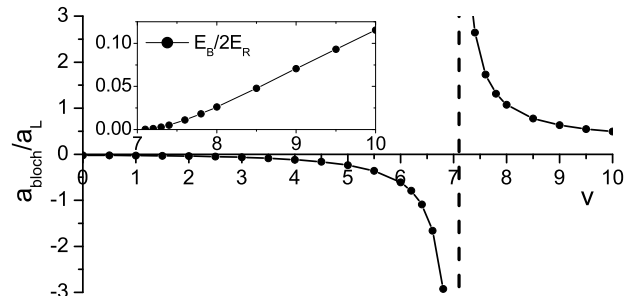


FIG. 3: Scattering lengths for collisions between  $^{87}\text{Rb}(b)$  and  $^{40}\text{K}(f)$  in optical lattices. The lattice wavelength  $\lambda = 755\text{nm}$  is chosen such that the potential depths measured by their respective recoil energies ( $E_{Rb}$ ,  $E_{Rf}$ ) are equal,  $v_b = v_f = v$ [18]. Vertical dashed line denotes the resonance scattering at  $v_c = 7.1$ . Inset is the two-body binding energy  $E_B$  in units of  $2E_R = E_{Rb} + E_{Rf}$  above resonance.

For ultracold isotopes with negative zero-field s-wave scattering lengths  $a_s$  such as  $^{85}\text{Rb}|2, 2\rangle$  ( $-390a_0$ ),  $^{39}\text{K}|1, 1\rangle$  ( $-45a_0$ ) and  $^7\text{Li}|2, 2\rangle$  ( $-27a_0$ ), using the lattice spacing as in [18] we find the onset of resonance at  $v_c = 5.5, 10.0, 11.7$  respectively. Fig.3 further shows the resonance scattering of  $^{87}\text{Rb}|1, 1\rangle \otimes ^{40}\text{K}|\frac{9}{2}, -\frac{9}{2}\rangle$  (inter-species scattering length  $a_{bf} = -177a_0$ ) at  $v_c = 7.1$ .

Two remarks are in order. First, for a weak s-wave interaction,  $|a_s| \ll \frac{a_L}{C_1}$ , the effective potential  $U_{\text{eff}}$  which is barely renormalized by higher bands can be simply related to the on-site interaction  $U$  in the Bose-Hubbard model,  $\frac{U_{\text{eff}}}{\Omega} = \frac{U}{N_L}$  ( $\Omega = N_L a_L^3$ ). In this case  $v_c \gg 1$ ; following Eq.(5-7),  $a_{\text{bloch}}$  can then be expressed as

$$\frac{a_{\text{bloch}}}{a_L} = \frac{1}{4\pi} \left( \frac{t}{U} + \frac{\gamma}{16} \right)^{-1}, \quad (9)$$

that is consistent with results in Ref.[13] and predicts a resonance at  $\frac{t}{U} \approx -0.25$ . Second, when using the RG approach to calculate effective interaction within the lowest transverse mode in 1D waveguides, we get identical results as obtained by using pseudopotentials[6].

We also studied the low-energy scattering matrix  $T_0(E)$  for two atoms with total energy  $E$ [17]. Using similar diagrams as shown in Fig.1 we express  $T_0^{-1}(E) = T_0^{-1}(0) + \frac{m}{4\pi a_L} f(E)$ , to get which all  $\epsilon_{n\mathbf{k}}$  in Eq.(5-6) are replaced with  $\epsilon_{n\mathbf{k}} - E/2 - i0^+$ . It is convenient to introduce a dimensionless energy,  $\tilde{E} = E/2t$ . Fig.4 shows both real ( $f_R$ ) and imaginary ( $f_I$ ) components of  $f(\tilde{E})$  for  $v = 4$ . The variation of  $f_R$  is mainly due to the intraband

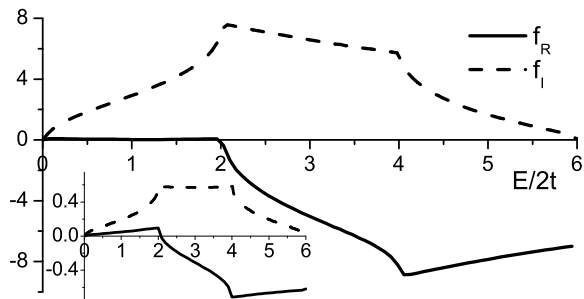


FIG. 4: Real( $f_R$ ) and imaginary( $f_I$ ) components of  $f(E)$  in an optical lattice with depth  $v = 4$  (the lowest band width  $6t = 1.03E_R$ ). Inset shows results multiplied by  $t/2E_R$  in a single-band approximation.

scattering.  $f_I$  is related to the normalized density of state  $\rho(\tilde{\epsilon})$  via  $f_I = 4\tilde{E}_R\rho(\frac{\tilde{E}}{2})$ . An exact particle-hole symmetry in the lowest band would result in the following relations,  $f_R(\tilde{E}) + f_R(6 - \tilde{E}) = f_R(6)$  and  $f_I(\tilde{E}) = f_I(6 - \tilde{E})$  (see inset in Fig.4). The deviations from these symmetries in our data can be ascribed to the imperfect symmetry of the lowest band, and most importantly interband scattering effects. Finally, compared with free space results where  $f_R = 0$  and  $f_I \propto \sqrt{E}$ , the T-matrix in optical lattices exhibits a much richer low energy  $E$ -dependence.

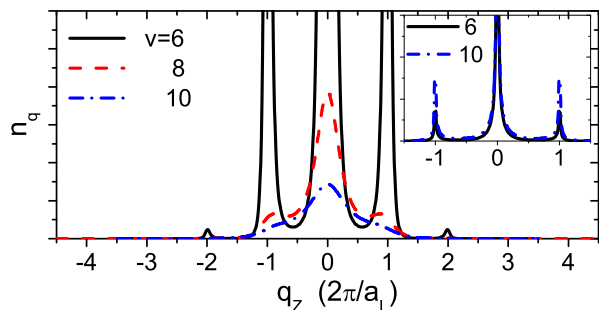


FIG. 5: (color online). Real momentum distribution  $n_{\mathbf{q}}(q_x = q_y = 0, \text{normalized})$  of bound states in optical lattices at different depths  $v(> v_c)$ . The s-wave scattering length is  $a_s = -0.05a_L$  and correspondingly the resonance occurs at  $v_c = 5.6$ . Inset is for a dilute cold bosonic gas with  $a_s = 0.05a_L$ , where multiple peaks at discrete reciprocal lattice momenta are due to condensates.

Beyond  $v_c$ , a stable molecule is formed with a binding energy  $E_B(> 0)$  that satisfies a two-body equation as

$$-\frac{\Omega}{U_0} = \frac{M}{\eta(E_B)} \sum_{n=0, \mathbf{k}} \frac{1}{2\epsilon_{n\mathbf{k}} + E_B} + \sum_{n>0, \mathbf{k}} \frac{1}{2\epsilon_{n\mathbf{k}} + E_B} \quad (10)$$

Further increasing  $v$  above  $v_c$  leads more localized and tightly-bound molecules, which could be experimentally detected by measuring  $E_B$  or probing the momentum distribution ( $n_{\mathbf{q}}$ ) after free space expansion. For a two-body bound state constructed

as  $|\Psi\rangle = \sum_{n\mathbf{k}} c_{n\mathbf{k}} \psi_{n\mathbf{k}}^\dagger \psi_{\mathbf{n}-\mathbf{k}}^\dagger$ , one can get  $n_{\mathbf{q}} = \sum_{n\mathbf{k}\mathbf{G}} \delta_{\mathbf{q}, \mathbf{k}+\mathbf{G}} |w_n(\mathbf{k} + \mathbf{G})|^2 |c_{n\mathbf{k}}|^2$ . In Fig.5 we plot  $n_{\mathbf{q}}$  along  $z$ -axis for different  $v > v_c$ . We find that for the dominating lowest band, the probability function ( $|c_{0\mathbf{k}}|^2$ ) spreads more uniformly over  $BZ$  as  $v$  is increased. This directly leads to a smeared multi-peak structure and a more extended range of  $n_{\mathbf{q}}$ , which is expected to eventually follow a smooth Gaussian distribution of  $w_0(\mathbf{q})$ .

In conclusion, we have studied the low-energy effective scattering between Bloch waves in optical lattices. The resonance scattering induced by intraband or interband effects offers an alternative path to unitary cold Bose gases so far mainly studied via Feshbach resonances[19, 20]. These lattice resonances can also be utilized to study exciting few-body physics of heteronuclear molecules and Efimov states. This work is in part supported by NSFC, 973-Project (China), and by NSERC (Canada), Canadian Institute for Advanced Research.

- 
- [1] E. Tiesinga *et al*, Phys. Rev. A **47**, 4114 (1993); J. P. Burke *et al*, Phys. Rev. Lett. **81**, 3355 (1998).
  - [2] S. Inouye *et al*, Nature **392**, 151 (1998); Ph. Courteille *et al*, Phys. Rev. Lett. **81**, 69 (1998); J. L. Roberts *et al*, Phys. Rev. Lett. **81**, 5109 (1998).
  - [3] T. Busch *et al*, Found. Phys. **28**, 549 (1998).
  - [4] T. Stöferle *et al*, Phys. Rev. Lett. **96**, 030401 (2006).
  - [5] C. Ospelkaus *et al*, Phys. Rev. Lett. **97**, 120402 (2006).
  - [6] M. Olshanii, Phys. Rev. Lett. **81**, 938 (1998); T. Bergeman *et al*, Phys. Rev. Lett. **91**, 163201 (2003).
  - [7] H. Moritz *et al*, Phys. Rev. Lett. **94**, 210401 (2005).
  - [8] D. S. Petrov *et al*, Phys. Rev. Lett. **84**, 2551 (2000); D. S. Petrov *et al*, Phys. Rev. A **64**, 012706 (2001).
  - [9] M. Greiner *et al*, Nature **415**, 39 (2002).
  - [10] M. Köhl *et al*, Phys. Rev. Lett. **94**, 080403 (2005).
  - [11] J. K. Chin *et al*, Nature **443**, 961 (2006).
  - [12] O. Mandel *et al*, Nature **425**, 937 (2003).
  - [13] P. O. Fedichev *et al*, Phys. Rev. Lett. **92**, 080401 (2004).
  - [14] The specific scheme here is equivalent to a more general systematic approach to two-body scattering originally proposed in D. B. Kaplan *et al*, Nucl. Phys. B **534**, 329 (1998).
  - [15] Numerical results show that intraband interactions have very weak dependences on  $\mathbf{k}, \mathbf{k}'$ .  $M$  obtained for  $\mathbf{k} = \mathbf{k}' = \mathbf{0}$  follows  $1 + \frac{3v^2}{32}$  and  $(\frac{\pi}{2})^{\frac{3}{2}} v^{\frac{3}{4}}$  respectively in the small and large  $v$  limit.
  - [16]  $\eta$  depends on both  $a_s$  and  $v$ . Given a negative  $a_s$ ,  $\eta$  initially increases from unity with  $v$  but finally decreases in the large  $v$  regime. The amplitude of  $\eta$  depends on  $a_s$  and is negligible for small  $|a_s|$ . Even for large  $|a_s|$ ,  $\eta = 1$  is still valid near resonances.
  - [17] C. J. Pethick and H. Smith, *Bose-Einstein Condensation in Dilute Gases*, Cambridge University Press, Cambridge (2002).
  - [18] Th. Best *et al*, Phys. Rev. Lett. **102**, 030408 (2009).
  - [19] S. B. Papp *et al*, Phys. Rev. Lett. **101**, 135301 (2008).
  - [20] S. E. Pollack *et al*, Phys. Rev. Lett. **102**, 090402 (2009).